ELSEVIER

Journal of Structural Geology 29 (2007) 1131–1147

JOURNAL OF STRUCTURAL GEOLOGY

www.elsevier.com/locate/jsg

# The high P/T Sambagawa extrusional wedge, Japan

Soichi Osozawa [a,*], Terry Pavlis [b]

[a] *Department of Earth Sciences, Graduate School of Science, Tohoku University, Sendai 980-8578, Japan*
[b] *Department of Geological Sciences, University of Texas at El Paso, El Paso, TX 79968, USA*

Received 12 October 2006; received in revised form 22 March 2007; accepted 22 March 2007
Available online 4 April 2007

**Abstract**

A metamorphic inversion along the Asemigawa section of the Besshi unit in the Sambagawa high P/T metamorphic zone has been explained previously by S-vergent major recumbent folding or thrusting. Through careful structural field investigations, however, we recognize the D2 Asemigawa detachment fault at the boundary of the highest-grade (oligoclase–biotite zone) thermal culmination in the belt. We have also discovered a series of normal faults in the hanging wall of the major detachment in the upper domain and a series of thrust faults bounding every metamorphic mineral zone of the footwall in the lower domain. Outcrop-scale D2 asymmetric folds are closely associated with axial-planar pressure-solution cleavages, and are genetically related to the above D2 normal faulting and thrusting as fault-propagation folds. Northward fold vergence is found only in the upper domain and southward vergence is found only in the lower domain. Exceptions to this rule occur only for parasitic folds in the overturned limbs of mesoscopic folds, which indicates flexural slip as a likely fold mechanism. We propose an extrusion wedge model for the inverted metamorphism and accordingly, this mechanism may also account for a large part of the exhumation of the Sambagawa metamorphic rocks, although westward shear at the time of D1 stretching lineation has partly contributed to the exhumation by counter-flow in the accretionary wedge. We infer that M1 with its retrograde actinolite schists represents a D1 ductile shear zone, but it contributes as much as a component of the D2 Asemigawa detachment, other normal and thrust faults, and asymmetric folds, as reactivated brittle shear zones. Thus, shear direction had changed orthogonally and drastically between ductile D1 stretching and ductile–brittle transition to brittle D2 extrusion. We infer that this transition reflects the collision of an actively spreading mid-ocean ridge and is a consequence of increased coupling of plates and orogen-normal stress, followed by oblique subduction. D0 and $D_{-1}$ record eastward down-flow during the oblique underthrusting of oceanic plate, before peak metamorphism M1.


*Keywords:* High P/T; Sambagawa; Exhumation; Detachment; Counter-flow; Actinolite

## 1. Introduction

The Sambagawa zone (Fig. 1) is one of the most investigated high P/T metamorphic zones in the world. Investigations include many structural, petrological, and geochronological studies (e. g., Banno et al., 1978; Faure, 1985; Higashino, 1990; Takasu and Dallmeyer, 1990; Wallis, 1990; Enami et al., 1994; Okamoto, 1998; Osozawa, 1998; Yagi and Takeshita, 2002).

The Sambagawa high P/T zone represents an ancient subduction zone (Ernst, 1988). The Sambagawa complex originated as an accretionary complex (Okamoto et al., 2000), but has been buried much deeper than many other accretionary complexes that have been recognized at subduction zones outside of continental collision zones. The mechanism and process by which the high P/T rocks are exhumed from ~35 km (~10 kb) (e.g., Enami et al., 1994), however, remains unresolved. One model is that the higher-grade metamorphic rocks are sandwiched between lower-grade rocks by thrust and normal faults, and the high P/T rocks might have been squeezed from depth to the surface (Maruyama et al., 1996). This extrusion wedge model provides one mechanism for exhuming high P/T rocks (Ring and Reischmann, 2002; Schoonover and Osozawa, 2004). However, this process is only theoretical for the Sambagawa rocks (Wallis, 1998), and

* Corresponding author. Tel.: +81 22 795 6619.
*E-mail address:* osozawa@mail.tains.tohoku.ac.jp (S. Osozawa).

0191-8141/$ - see front matter © 2007 Elsevier Ltd. All rights reserved.
doi:10.1016/j.jsg.2007.03.014

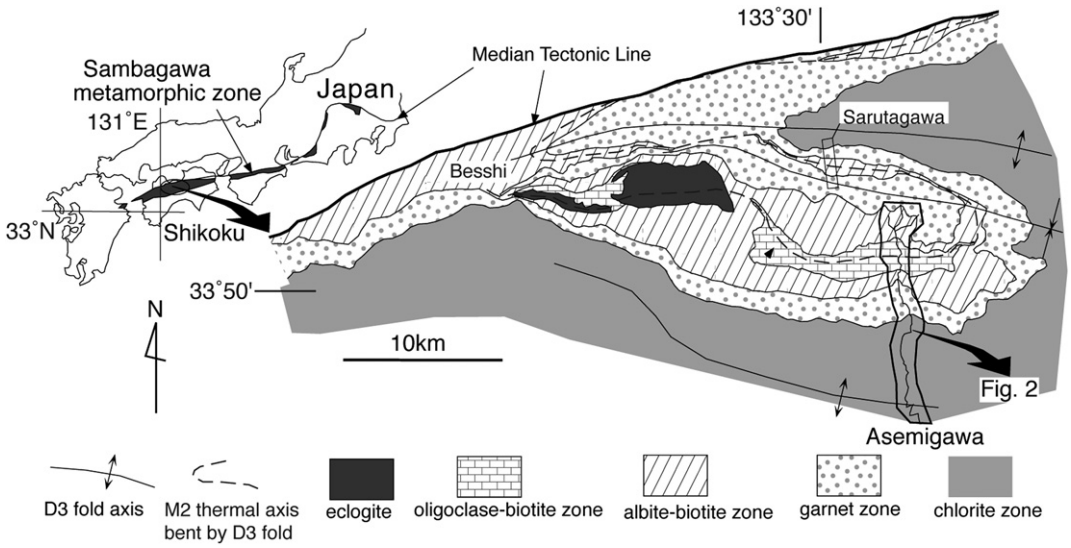


Fig. 1. The Sambagawa high P/T metamorphic zone, and mineral zones (after Higashino, 1990). D3 upright folds modify the distribution of mineral zones and the M2 thermal axis, and hence the extrusion wedge. Modified after Osozawa et al. (2006), fig. 1.

a detachment fault, which is explicitly predicted by the model has not been previously documented (Yagi and Takeshita, 2002; Takeshita and Yagi, 2004). Here, we present the results of field based and microstructural observations that provide new constraints on the ductile–brittle deformational history and provide support for the extrusional wedge model. Such constraints include new recognition of the Asemigawa detachment fault and a series of major thrust faults, both of which define the Sambagawa extrusion wedge.

## 2. Geological setting

The Sambagawa high P/T zone extends across most of southwest Japan (Fig. 1). It is bounded to the north by the low P/T Ryoke metamorphic zone and overlying Cretaceous Izumi Group along the Median Tectonic Line, and by the Mikabu and northern Chichibu zones to the south. The Median Tectonic Line dips at 30 degrees to the north (Ito et al., 1996), and it is inferred to have originated as a detachment fault (e.g., Wintsch et al., 1999). The Mikabu and northern Chichibu zones experienced the same thermal regime, but lower grade metamorphism than the Sambagawa zone (e. g., Suzuki and Ishizuka, 1998) and the structural relations are not yet constrained.

The Sambagawa zone consists of two units, the higher-grade, overlying Besshi unit and lower-grade, underlying Oboke unit. The Oboke unit is, however, restricted to Shikoku island. The Oboke rocks are thought to be the metamorphosed and exhumed Shimanto accretionary complex (e. g., Osozawa, 1998). The Besshi unit consists of metamorphosed basalt and basaltic tuff (mafic schist), mudstone (pelitic schist), sandstone (psammitic schist), and chert (quartz schist). The Oboke unit consists of metamorphosed sandstone, mudstone, and conglomerate.

An inverted metamorphic field gradient exists in the Besshi unit of the Sambagawa zone on Shikoku (Banno et al., 1978). Excellent exposures through these E–W trending structures are seen along the Asemigawa River, running N–S (Fig. 1). Metamorphic zones are defined by the first appearance of garnet, biotite, and oligoclase in pelitic and psammitic schists (Higashino, 1990). Relict plagioclase is restricted to the southern chlorite zone. Amphiboles in hematite-bearing metabasites change from actinolite to winchite and crossite to barroisite and hornblende, corresponding to increasing metamorphic grades of mafic schist (Otsuki and Banno, 1990). The prograde metamorphic conditions of the Asemigawa section are at 5.5–6.5 kb and $<360$ °C in the chlorite zone, 7–8.5 kb and 440 °C in the garnet zone, 8–9.5 kb and 520 °C in the albite–biotite zone, and 10–11 kb and 610 °C in the oligoclase–biotite zone (Enami et al., 1994). The highest-grade rocks in the oligoclase–biotite zone appear in the upper reaches of the river, but are in the middle of the structural sequence. That is, both upstream (northward) and downstream (southward) the rocks decrease in grade to the albite–biotite, garnet, and chlorite zones (Figs. 1, 2). The northward-dipping upper and lower sections along the river, which include both these normal and inverted metamorphic gradients, is the subject of this investigation.

Cooling ages from Besshi unit rocks are 80 Ma in Shikoku (muscovite Ar–Ar ages of the garnet, albite–biotite, and oligoclase–biotite zones; Takasu and Dallmeyer, 1990). The ages become younger northeastward in the Sambagawa zone in southwest Japan, and this diachronous cooling and exhumation is a consequence of cooling following the migrating trench–trench–ridge triple junction in the Late Cretaceous to Paleogene (Osozawa, 1998). Ridge subduction induced shortening of the volcanic arc and fore-arc, and exhumed low and high P/T metamorphic rocks (the Ryoke and Sambagawa rocks) and plutonic rocks (Osozawa, 1998). However, the exact process of exhumation or the deformation associated with it is as yet unclear. Nonetheless, this problem is not significant in the present paper which addresses the older exhumation structure of the Besshi unit of the Sambagawa metamorphic zone.

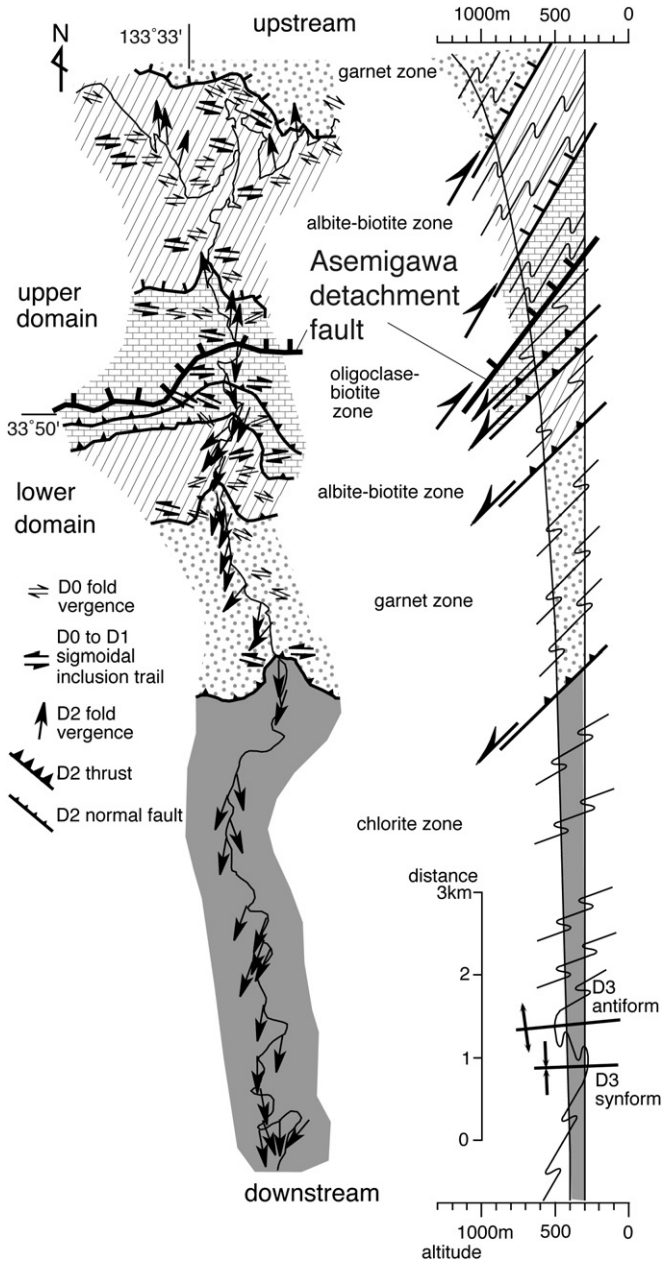


Fig. 2. Structural map (left) and cross section (right) along the Asemigawa River. Modified after Osozawa et al. (2006), fig. 3.

## 3. Structures of Besshi unit

Field investigations have revealed the presence of a hitherto unrecognized detachment fault in the oligoclase–biotite zone of the Asemigawa section, here referred to as the Asemigawa detachment. This ~E–W striking detachment separates two structural/metamorphic domains: (1) an upper domain, in the higher part of the Asemigawa drainage valley, contains a normal metamorphic gradient with normal faults developed subparallel to foliation and associated north-vergent asymmetric folds; and (2) a lower domain with an inverted metamorphic gradient, numerous thrust faults, and south-vergent asymmetric folds. The major faults described here within this section have not been previously recognized and their presence between every metamorphic mineral zone of the Asemigawa section is critical to the inferred exhumation history. The faults formed under brittle to brittle–ductile transition conditions are all assigned to N- or S-directed D2, which overprints W-directed ductile D1 structures; a relationship that requires complete re-evaluation of previous structural models.

We have divided the deformation phases into five events, D minus 1 ($D_{-1}$), D0, D1, D2 and D3, based on the overprinting relationships observed in outcrops and thin sections. A stretching lineation is developed during D1, and provides a good reference for comparison with previous work. Our D1 is equivalent to D1 of Faure (1983, 1985), Hara et al. (1992), Nishikawa et al. (1994), and others. Wallis (1990, 1995, 1998; Wallis et al., 1992), however, combined D1 and D2 into a single deformational phase, but we show below that this conclusion is inconsistent with new data. Clarification of this sequence is important because differing interpretations have confused later structural studies like Okamoto (1998), Wintsch et al. (1999), Abe et al. (2001), and Yagi and Takeshita (2002).

For describing $D_{-1}$, D0, D1, and some D2 minor structures, we use the standard terminology of X = maximum principal finite stretch axis, Y = intermediate axis, and Z = short axis, inferred from D1 schistosity and lineation. The horizontal X axis trends E–W, and the Y axis plunges to the north (Fig. 3A). Metamorphic events corresponding to $D_{-1}$, D1, and D2 are labeled $M_{-1}$, M1, and M2 respectively. We also examined fold asymmetry as an indicator of shear sense and use the term vergence to describe the inferred long-limb over short-limb shear sense and we use the term without regard to facing.

As an introduction to our interpretation of the structural history, we suggest that $D_{-1}$ and D0 phase occurred at brittle–ductile transition conditions, probably reflecting E-directed underthrusting and down-flow of a corner-flow system (Cloos, 1982). The following D1 phase records ductile flow under prograde conditions, but includes the subsequent retrograde M1 phase, probably reflecting underplating and partial exhumation, and also westerly, thrust-directed counter-flow in a corner-flow system. The D2 phase occurred under more or less brittle conditions, strongly reflecting exhumation and S-directed wedge-extrusion orthogonal to the previous kinetic directions, and also reflecting strong coupling of overriding and subducting plates behind the triple junction (Osozawa, 1998).

### 3.1. D0 and $D_{-1}$

D0 micro folds are found in thin section, but are restricted to plagioclase porphyroblasts; which occur in pelitic schists of the oligoclase–biotite, albite–biotite, and garnet zones (Fig. 4A). Wallis (1998) also reported this D0 folding (in his labeling; Dr). The margin, or rim of the porphyroblasts, cuts the folds (Fig. 4A), which indicates that the micro folding pre-dates the growth and formation of D1 plagioclase porphyroblasts. The foliation, which defines the D0 folds and labeled

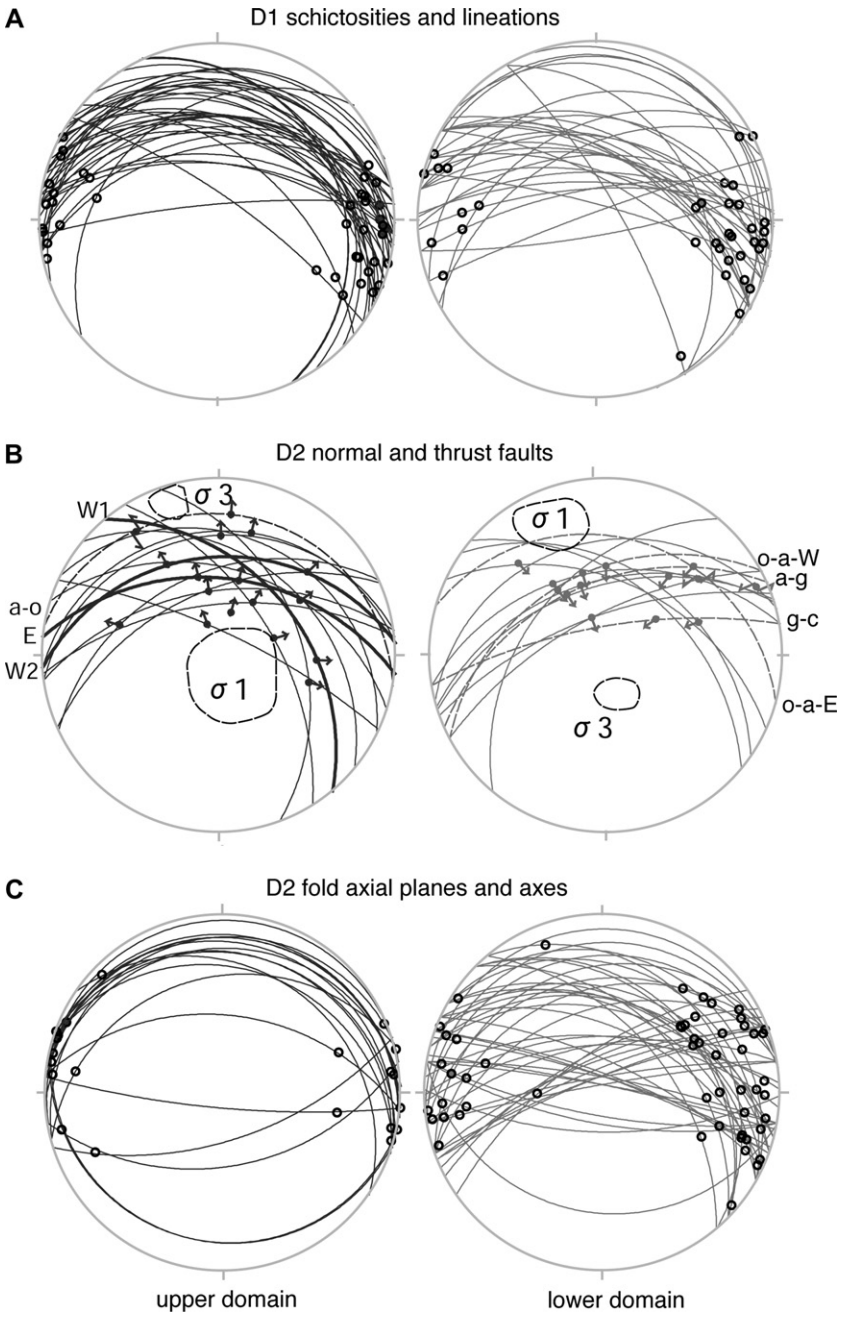


Fig. 3. Lower hemisphere and equal area projections of: (A) D1 schistosities and stretching lineations, (B) D2 normal and thrust faults, and estimated stress fields, (C) D2 fold axial planes and axes, in the upper and lower domains. The higher and lower angles of D2 axial planes relative to D1 schistosities reflect their N- and S-vergent directions, respectively. Panel B modified after Osozawa et al. (2006), fig. 4.

D minus 1 ($D_{-1}$), is composed of thin alternating layers of opaque minerals and very fine-grained white micas. The character of this foliation suggests it formed by pressure solution, and the inference of pressure solution suggests that $D_{-1}$ occurred under brittle–ductile transition conditions. The $D_{-1}$ white mica layers are clearly bent by the D0 folding, and do not define the D0 axial surfaces. The $D_{-1}$ mica and opaque mineral fabric is thus clearly distinguished from much coarser-grained D1 fabric outside of porphyroblasts (Fig. 4A). The $D_{-1}$ and D0 fabric is sometimes dissolved and obscured in the sub-grained margin of porphyroblasts.

The D0 folds are Class 1B to 1C (Ramsay, 1967; Fig. 4A) folds. The folds are open to tight, with curviplanar axial surfaces, even within a porphyroblast (Fig. 4A). D0 folds are asymmetric and exhibit a dominant eastward vergence in XZ sections (Figs. 2, 4A, 5A). This sense of asymmetry is consistent within 26 thin sections that contained D0 folds (Fig. 2). In YZ sections, the $D_{-1}$ foliations locally form eye-structures (Fig. 5B), while in XY sections, the $D_{-1}$ foliations are orthogonal to the X axis, or tend to be convex eastward (Fig. 5C). These three dimensional observations may indicate that the D0 folds are east-verging sheath folds, accompanied by

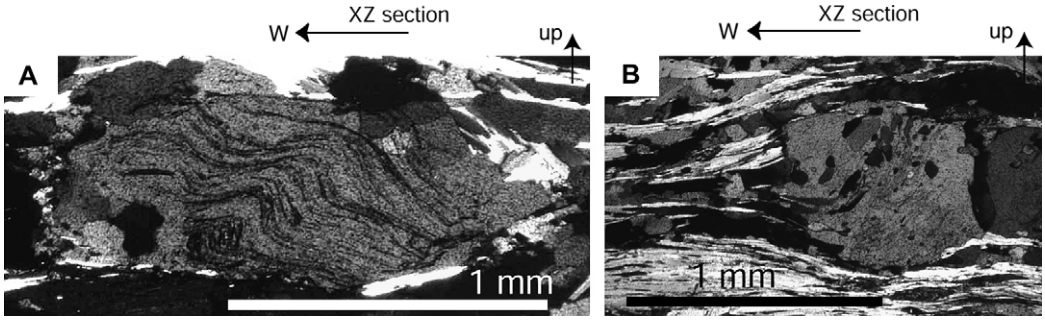


Fig. 4. (A) D0 micro folds with eastward vergence in pelitic schist. (B) $D_{-1}$ planar inclusion trails in the core of a D1 porphyroblast in mafic schist, with part of the sigmoidal inclusion trails indicating westward D1 shear. Both are in the XZ section, from northern albite–biotite zone, and in cross-polarized light.

top-to-the-east shear, although interpretations of shear senses from fold asymmetry can be ambiguous (Carreras et al., 2005). D0 and D1 appear to share the same stretching X axis. It is important to reiterate that the D0 eastward shear is consistent throughout the Asemigawa section (Fig. 2), and that it is unrelated to the D2 metamorphic inversion. We observe four exceptions (Fig. 2) that are all located on the overturned limbs of D2 folds. Also the porphyroblasts apparently have overgrown the D0 structures and protected them from modification during severe overprinting by D1 shearing. However, the $D_{-1}$ foliations and D0 fold axial surfaces tend to dip westward relative to D1 foliations (Figs. 4A, 5A), which suggests an effect of rotation of porphyroblasts and hence W-directed D1 shear.

Within mafic schists, D1 plagioclase porphyroblasts show similar $D_{-1}$ fabrics preserved as a preferred orientation in amphibole and epidote (Fig. 4B; Takeshita et al., 2005; their $S_i$ in an S-shaped inclusion trail). The $D_{-1}$ fine-grained calcic amphibole has lower Al content than D1 coarse-grained matrix amphibole, suggesting a relatively lower metamorphic temperatures for $D_{-1}$ (Takeshita et al., 2005), and these amphiboles are easily distinguishable in thin section. However, the D0 fabric is only planar or sigmoidal (Fig. 4B), and unlike porphyroblasts in pelitic schist, shows no sign of D0 asymmetric folding.

### 3.2. D1

A schistosity, a stretching lineation and sheath folds were all produced during D1. For pelitic and psammitic schists, the schistosity consists of an alternation of quartz- and mica-rich layers. For the higher grade rocks, plagioclase and garnet D1 porphyroblasts are included in quartz-rich layers. For mafic schists, M1 amphibole and pyroxene form the schistosity.

In XZ sections, mica, sub-grained quartz, plagioclase porphyroblasts, chlorite, amphibole, and pyroxene have long axes aligned parallel to the schistosity (Fig. 5A). In YZ sections, these minerals are round or square-shaped and surrounded by micas (Fig. 5B). Mica layers are sometimes crenulated, but crenulation in some layers is discontinuous. We refer to this type of crenulation as D2, and infer that it is a pressure solution cleavage, although Faure (1983, 1985) and Abe et al. (2001) labeled this crenulation D1. In XY sections, these and opaque materials are aligned parallel to the X stretching axis, while sub-grained quartz and chlorite are elongated forming pressure shadows, and rectangular minerals, like apatite, are pulled apart (Fig. 5C). This D1 lineation is also preserved in hand specimens in the schistose foliation. D2 crenulations form an intersection lineation on the D1 foliation almost parallel to the D1 lineation, but sometimes sufficiently oblique so that the lineations can be distinguished (see below).

The D1 lineation is therefore a stretching and mineral lineation. The observed D1 strain is constrictional, which is consistent with a study using radiolarians as strain markers (Toriumi, 1985), although inconsistent with inferences by Moriyama and Wallis (2002) and Takeshita and Yagi (2004). D1 sub-grained quartz demonstrates constriction in rocks from the chlorite zone, in contrast to D2 sub-grained quartz, which is flattened perpendicular to D2 pressure solution

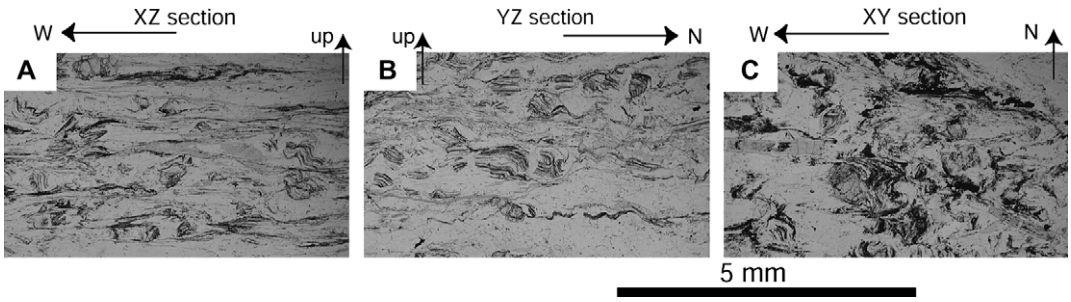


Fig. 5. (A) D0 micro fold and D1 schistosity in the XZ section, (B) D0 eye fold and D2 crenulation cleavage in the YZ section, and (C) D1 stretching lineation and pull apart of apatite in the XY section. Pelitic schist, northern albite–biotite zone, in cross-polarized light.

cleavage (Nishikawa et al., 1994; Takeshita and Yagi, 2004). Also we have measured constricted radiolaria in red chert of the Mikabu zone (X/Y = 2.32, Y/Z = 1.34), which underwent the same M1 metamorphism as the Sambagawa zone.

Shear bands, asymmetry of pressure shadows, and quartz shape- and lattice-fabrics have been reported in the Sambagawa zone (Wallis, 1990; Abe et al., 2001). Shear bands and lattice-fabrics were extensively measured (Tagami and Takeshita, 1998; Yagi and Takeshita, 2002; Takeshita and Yagi, 2004) from samples collected along the Asemigawa River and 25 of 27 samples showed top-to-the-west shear senses with the two opposite shear sense samples located on the overturned limbs of D2 folds.

Sigmoidal inclusion trails (Fig. 4B) in plagioclase porphyroblasts are observed in the XZ sections of mafic schists. The rims of the porphyroblasts are dissolved, reprecipitated, and stretched to form the D1 lineation (Takeshita et al., 2005), and they are interpreted to be syn-tectonic D1 porphyroblasts, although Takeshita et al. (2005) also considered that the core is an inter-tectonic porphyroblast which contains $D_{-1}$ planar inclusion trails. The anorthite content of porphyroblasts increases from core to rim (Enami, 1983), although the rim further records the retrogression as mentioned above. In the Sambagawa zone, this sigmoidal shape has been used to determine D1 shear sense (Takagi and Hara, 1979; Faure, 1983, 1985; Wallis, 1990, 1995, 1998; Wallis et al., 1992; Okamoto, 1998). Although Takeshita et al. (2005) stress that the sigmoidal inclusion trails are not strictly a diagnostic indicator of D1 shear sense because of the large differential rotations, the actually observed sigmoidal inclusion trails in 15 thin sections examined by us systematically dip to the west and hence suggest top-to-the-west shear throughout the Asemigawa section (Fig. 2). This sense is entirely consistent with the results of Tagami and Takeshita (1998) and Takeshita and Yagi (2004) from 16 samples analyzed for D1 lattice-fabrics for quartz. The shear sense is, like D0, unrelated to variations in metamorphic grade, and all exceptions to top-east shear sense (Fig. 2) are located on the overturned limbs of D2 folds.

D1 sheath folds are observed rarely in outcrop (Faure, 1983, 1985; Wallis, 1990). We also observed eye folds in regions within YZ sections of outcrop, suggesting sheath folding. The folds are similar in style, and closed to tight. On the microscopic scale, these folds are defined by the preferential arrangement of quartz- and mica-rich layers. The shape of the quartz and mica fabric, however, defines the axial plane and hence the overall D1 schistosity (Fig. 6A), as is typical with similar folds (Ramsey, 1967, pp. 429–430). These D1 fold axes are sub-parallel to D1 stretching lineations, an observation consistent with work by Nishikawa et al. (1994) in chlorite zone rocks of the region.

### 3.3. D2

#### 3.3.1. Relation of D2 folding and faulting, and M2 metamorphic conditions

D2 folds and faults are closely associated with each other, and additionally with axial planar cleavage, as commonly observed in the Japanese accretionary complexes (e.g., Schoonover and Osozawa, 2004). However, the mechanical relationship of these fold, fault, and cleavage systems has not been fully addressed in literature on the structural geology of the region, and thus, we first describe a typical outcrop (Fig. 7). We also highlight the coincidence of fold vergence and fault shear sense, and hence support the validity of using vergence to determine shear sense.

N-vergent asymmetric folds (S-shaped folds viewed to the east) are well exposed in the southern albite–biotite zone (Fig. 7A). These outcrop scale folds are parasitic to a south vergent higher-order macroscopic fold (Z-shaped fold), and are located in its corresponding overturned short-limb. The axial planes are parallel to the D2 cleavage and fault planes, and oblique to the D2 folded D1 schistosities. Some quartz veins are filling inter-layer space of folded D1 schistosities, and such dilation veining (Ramsay, 1967) is synchronous to the D2 folding (Fig. 7A). These veins are penetrated by the D2 spaced cleavages in the host rocks (Fig. 7B). In thin section,

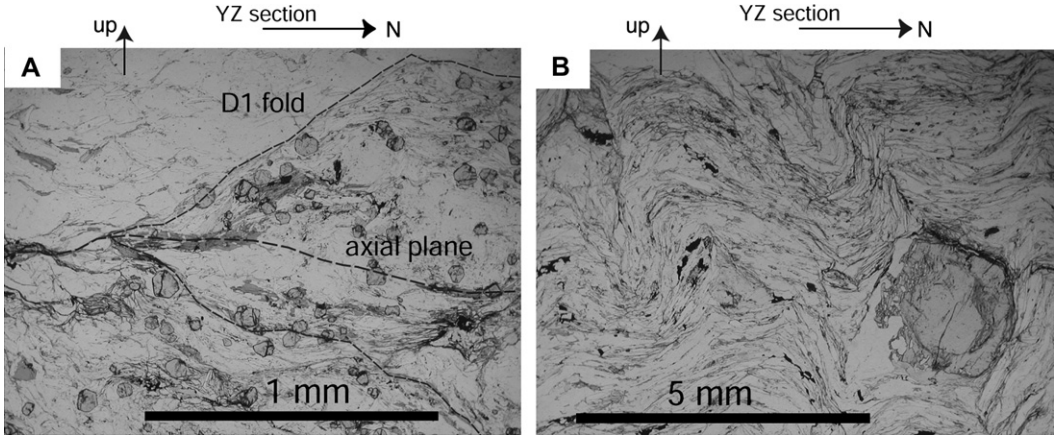


Fig. 6. (A) D1 sheath fold. Axial plane is defined by preferential arrangement of M1 micas (0001), and the fold deforms quartz- and mica-rich layers. Modified after Osozawa et al. (2006), fig. 13A. (B) D2 fold. Axial plane is defined by D2 pressure-solution cleavage, which crosscuts and bends D1 foliations. S vergence is same as the mesoscopic fold shown in Fig. 11A. Both are in the YZ section, from pelitic schist of oligoclase–biotite zone in the upper and lower domains, respectively, and in plane-polarized light.

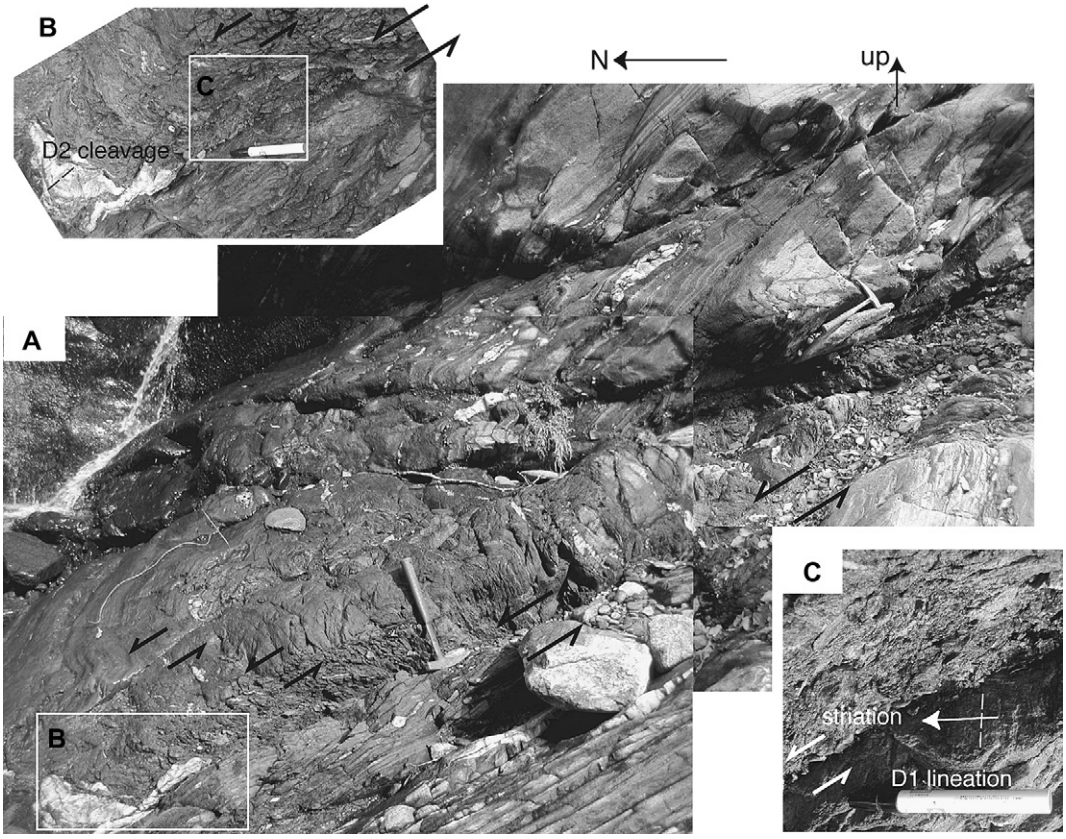


Fig. 7. D2 N-vergent asymmetric fold and associated N-thrown faults in an overturned limb. (A) Whole figure, (B) master gouge fault, and (C) striations on master fault. Pelitic schist of albite–biotite zone in lower domain. Panel A modified after Osozawa et al. (2006), fig. 12B.

these rough cleavages also can be called crenulation cleavages (e. g., Fig. 6B). Other than the master fault, minor faults with fault gouges are observed as well, typically offsetting D2 folded quartz veins several centimeters, top-down to the north (Fig. 7A), which is coincident with the inferred normal-slip shear-sense of N-vergent parasitic folds. The main normal fault also shows a prominent gouge zone which displays ''meteoric tails'' along striations that are consistent with top north-directed, normal sense, shear (Fig. 7C). The D2 striation is almost exactly orthogonal to D1 stretching lineation (Fig. 7C).

We infer that the S- and Z-shaped pattern of parasitic folds are a consequence of flexural slip acting on both limbs of the first-order buckled antiform–synform pair. Open space formed by flexural slip was filled by quartz veins, which were further shortened by axial–planar cleavage development, hence buckling and pressure solution acted progressively. Flexural-slip, which provoked secondary, antithetic N-directed flexural shear, is expressed in S-shaped asymmetric folds and N-directed gouge-bearing brittle faults. The master thrust fault is not exposed. However, this first-order antiform and associated synform is expected in the hanging-wall of a brittle thrust to the south and, therefore, the first-order fold can be called fault-propagation fold following the model of Suppe (1985). The folding, pressure solution, and faulting are thus a consequence of pure shear overprinting a simple shear component. The asymmetry of the first-order fold and S-directed thrusting is explained by large-scale simple shear.

Constraints on the metamorphic or sub-metamorphic conditions of D2 or M2, which is estimated to be less than 2.5 kb and 250 °C, are as follows:

1. M1 peak metamorphism in the chlorite zone is at 5.5–6.5 kb and less than 360 °C (Enami et al., 1994).
2. Temperature inferred from quartz brittle deformation is less than 300 °C (e. g., Passchier and Trouw, 1996), contrasting to the estimated 300–400 °C for D1 lattice-fabric of quartz (Tagami and Takeshita, 1998; Yagi and Takeshita, 2002; Takeshita and Yagi, 2004).
3. Prograde and retrograde D1 stretching and necking of amphiboles, of which the final product is actinolite, indicates a decrease of pressure and temperature from 10 kb and 550 °C to 4 kb and less than 300 °C (Wintsch et al., 1999).
4. M1 retrograde actinolite, which we discovered during this study, constitutes a major component of some D2 faults and folds, and such actinolite in metamorphosed ultramafic rocks indicates sub-greenschist facies of ca. 2.5 kb and 250 °C (Spear, 1993; Robinson et al., 1981).
5. M2 white micas recrystallized by D2 pressure solution are not recognized in any thin section, and the M2 temperature is therefore less than 300 °C.
6. Our illite crystallinity data (Frey and Robinson, 1999) of probable retrograded M1 white micas (Radvanec et al., 1994) suggests a temperature of ~300 °C using calibrations provided by Underwood et al. (1993).

7. D2 folds are parallel folds and kink folds, consistent with low-T brittle–ductile deformation during folding.
8. D2 striations formed by flexural slip are sometimes observed on folded surfaces, orthogonal to the D2 fold axis.
9. Faults show accompanying fault striation and gouge consistent with low-T brittle conditions.

### 3.3.2. The Sambagawa extrusion wedge and domain division

The upper and lower domains are separated by the D2 Asemigawa detachment fault, and their internal structures, normal vs. thrust faults, N vs. S directed folds, and M2 right way up vs. inverted thermal structures, are distinct across the fault.

Palaeostress fields were estimated using the multiple inverse method on the brittle fault arrays in each domain (Yamaji, 2000, 2003). In line with the observed faults, this analysis shows that the upper domain is characterized by a NNE-directed horizontal minimum stress and vertical maximum stress as the dominant paleostress (Fig. 3B), while the lower domain exchanges these stress axes (Fig. 3B). Under these inferred paleostress fields, normal faults in the upper domain propagate downward, and thrust fault in the lower domain propagate upward. This propagation produces a crustal-scale antiform or extrusion wedge (Grujic et al., 1996). At local scales, however, the D2 fold style observed suggests flexural-slip folding (see above), and not a shear fold as predicted by Grujic et al. (1996). Nonetheless, the model by Grujic et al. (1996) referred to the large-scale shear within the system and not necessarily to the details of accommodation of the deformation, and the key relationship is the reversal in shear sense within the extrusional wedge. Thus, the structural description in this paper is a partly modified definition of an extrusion wedge where the shear is accommodated by a combination of penetrative strain, asymmetric folding of older foliations, and brittle faults.

### 3.3.3. Asemigawa detachment fault

The newly named Asemigawa detachment fault is exposed in the axial part of the oligoclase–biotite zone, at the eastern and western ends of the mapped area in Fig. 2.

In the eastern outcrop (Fig. 8A,B), the hanging wall is psammitic schist and the footwall is pelitic schist, the latter corresponding to the metamorphic core. The shear zone is 50 cm wide, and consists primarily of actinolite schist (Fig. 8A). The actinolite crystals are several mm long, and the crystallographic c-axis forms the subhorizontal D1 stretching lineation. The mode of actinolite is ~90% (Fig. 8B corresponding to actinolite poorer part), and the rock composition is ultramafic, which is also indicated by the absence of albite. The actinolite schist additionally contains a small amount of probable relict biotite with retrograde chlorite replacement (Fig. 8B), and also talc and serpentine (Takeshita, T., personal communication, 2006). The absence of metamorphic olivine and pyroxene is another characteristic. The mineral assemblage indicates sub-greenschist facies only, considering the triangular phase diagram for the system $SiO_2$–MgO–CaO–$H_2O$ and reactions by Spear (1993, p. 475), and chrisotile + talc + tremolite paragenesis for prehnite–pumpellyte facies by Robinson et al. (1981, p. 100; table 13-2 in Spear, 1993 is after their table 6), although Si formula contents are 7.59–7.76 (Osozawa et al., 2006) less than expected 7.9–8.0 by Robinsin et al. (1981) and Spear (1993). The reaction of chrisotile + tremolite = antigolite + diopsite + $H_2O$ in Robinson et al. (1981, p. 100) is also critical for this low-grade metamorphism (although it is not shown in Spear, 1993). Hence, retrograde M1 was under such conditions, much lower temperature than those of the surrounding oligoclase–biotite zone, and followed by D2 faulting involving the M1 actinolite schist and M2.

The D2 shear planes are, however, observed and associated with high-angle N-plunging striations (Fig. 3B) and N-vergent asymmetric folds (Fig. 3C), both of which show N-directed (normal slip shear sense) shear, including the upper and lower contacts of the actinolite schist (in Fig. 8A, for example, a marker bed is displaced along a minor shear plane). Lenticular quartz veins lie mostly along the shear plane, and are cracked parallel to the axial plane of D2 asymmetric folds. In YZ thin sections, such quartz veins show wavy extinction, and biotite crystals are affected by kink folding (Fig. 8B), both of which are parallel to mesoscopic D2 axial planes. The vein quartz is also overprinted by pressure solution at the sub-grain boundaries.

In the western outcrop, the Asemigawa detachment fault consists of a concave upward surface (Fig. 8C). The hanging wall is psammitic schist, and the footwall is mostly actinolite schist with lesser amounts of pelitic schist (Fig. 8C–E), and the actinolite schist is the main component caught up in the Asemigawa detachment fault (the lower contact is not exposed). As in the eastern exposure, actinolite is partly coarse-grained, shows E–W stretching, and contains additional biotite. The actinolite schist constitutes the brittle shear zone of the detachment and is more than 3 m thick (Fig. 8C). The master fault surface has fault gouge and N-directed striations (Fig. 3B). N-vergent folds are present in the shear zone schist and quartz veins as well as in the hanging wall schist, indicating N directed shear (Figs. 3C, 8C–E).

Yagi and Takeshita (2002) suggested the existence of a similar actinolite-bearing detachment fault at the Sarutagawa section, to the northwest of the Asemigawa section (Fig. 1), but the fault there occurs on the margin of the albite–biotite zone. They also report such actinolite-bearing faults from the Besshi area (Osozawa et al., 2006; Fig. 1).

### 3.3.4. Normal faults

D2 normal faults are common in the upper domain (Fig. 3B left). The boundary between the albite–biotite and oligoclase–biotite zones is also such a normal fault (Fig. 3B left, a-o).

The normal faults are accompanied by N-plunging striations (Fig. 3B left), and show a top-to-the-N shear sense based on the preservation of accretion steps (Fig. 9A). The fault zones contain black gouge cores a few millimeters to tens of centimeters in thickness, but mostly consist of

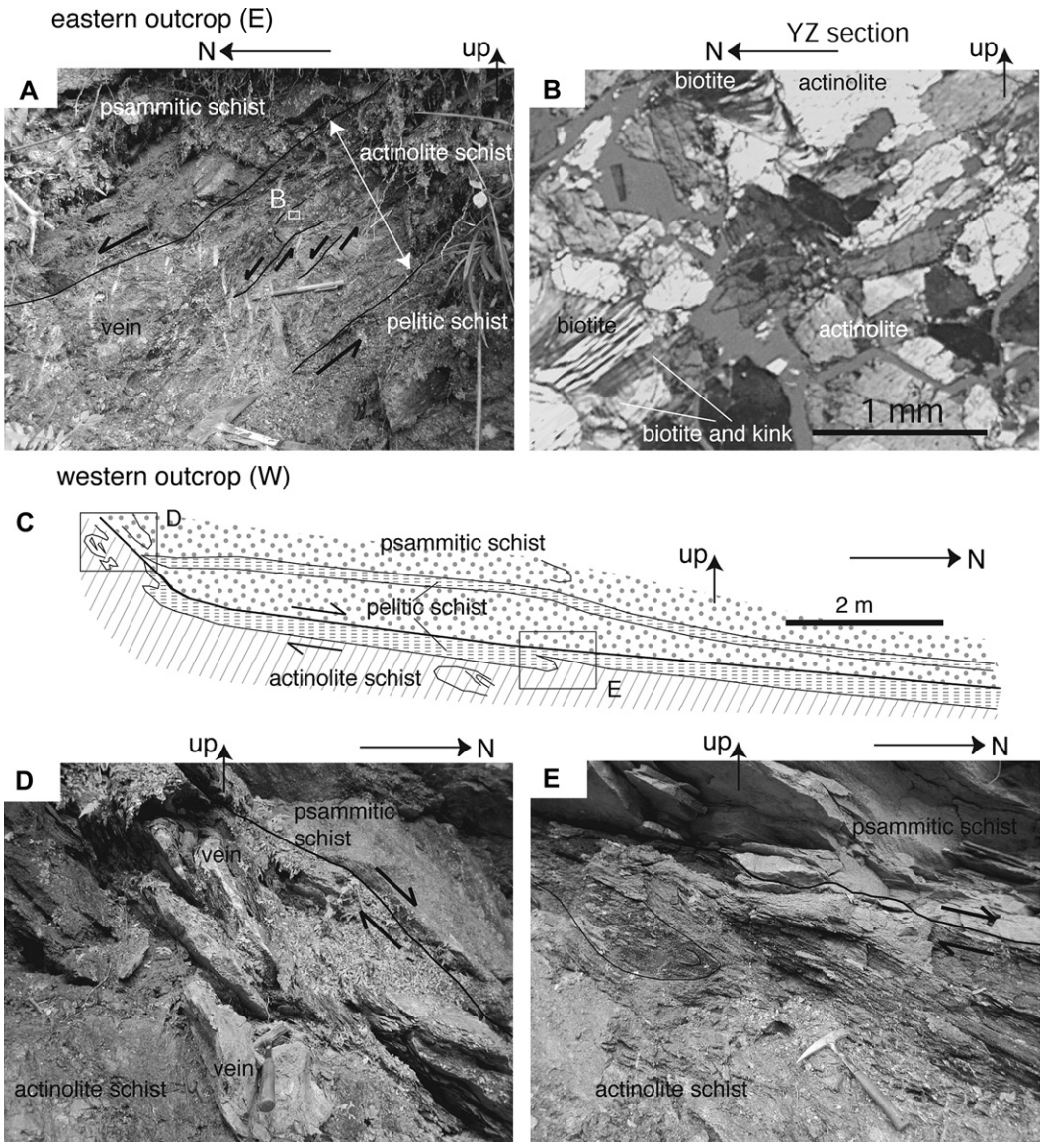


Fig. 8. The D2 Asemigawa detachment fault where it is exposed at the eastern outcrop (A: outcrop photo; B: thin section photo in small rectangle in photo A), and western outcrop (C: cross-sectional sketch; D,E: photos in rectangles in sketch C), within the mapped area. Modified after Osozawa et al. (2006), fig. 13B,D and fig. 11A–C, respectively.

a damage zone that produces a weathered schist. The main boundary fault has a shear zone ~1 m thick. The shear zone schist is commonly associated with N-directed asymmetric folds (Fig. 9B). A D2 fault propagation fold with N vergence is also observed in the schists of the hanging wall (Fig. 9C).

Takeshita and Yagi (2004) have reported conjugate sets of normal faults in the oligoclase–biotite zones, and their

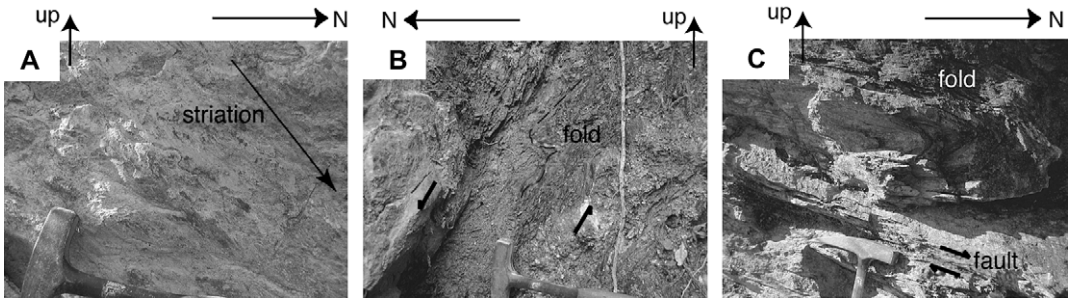


Fig. 9. D2 normal faults in upper domain. (A) Slickenlines and steps. (B) Asymmetric fold in shear zone (C) Normal fault propagation fold.

stress-axes projection (their Fig. 9) is similar to ours (Fig. 3B left), with a difference of their WNW- vs. our NNE-directed minimum stress. However, their data are obtained from the different area to the east of the Asemigawa section, and direct correlation is not possible. In addition, their normal faults have a large component of strike-slip, judging from their near-horizontal striation data (fig. 9 in Takeshita and Yagi, 2004). Similarly, we observed an equivalent strike-slip fault crosscutting the mafic schist mapped as a marker by Takeshita and Yagi (2004, fig. 10), and also a conjugate set of minor strike-slip faults. Such a conjugate set of strike-slip faults are known from the northern Shimanto zone (Osozawa, 1993). We labeled such strike-slip faults D3 (or D4). No conjugate relationship was observed for our D2 normal faults (Fig. 3B left).

### 3.3.5. Thrust faults

D2 thrust faults are widespread, but are restricted to the lower domain of the Asemigawa area (Fig. 3B). Three major thrust faults bound metamorphic mineral zones and, since these are newly recognized features, we describe them in detail here.

The thrust between the oligoclase- and albite–biotite zones (Fig. 2; Fig. 3B right, o-a-W; Fig. 10A) lies at the contact between the overlying mafic schist marker described by Takeshita and Yagi (2004) and underlying pelitic unit. The hanging wall is asymmetrically folded mafic and pelitic schist showing S vergence, and the footwall is pelitic schist only (Fig. 10A). An overturned synform, immediately above the master thrust (Fig. 10A), indicates a fault propagation mechanism for the D2 folding. The master thrust consists of actinolite schist ~20 cm thick (Fig. 10C). This lithological characteristic is again similar to fault rocks of the Asemnigawa detachment fault, showing that the thrusting is also D2 and that it occurred under extremely low metamorphic temperatures consistent with M2. The other shear zone is ~15 cm thick within footwall pelitic schist showing fault gouge, S-directed Riedel shears and minor displacement of a quartz vein (Fig. 10B). Overturned limbs are accompanied by parasitic N-directed asymmetric folds and asymmetric boudinage of quartz veins (Fig. 10D), showing the same, flexural slip-induced N-directed shear (cf. Fig. 7). This major thrust is traceable to the east (Fig. 3B right, o-a-E). The thrust here lacks actinolite, and instead consists of a 6 cm thick gouge zone within pelitic schist (Fig. 10E). The S-vergent synforms and antiforms are in the hanging wall and the marker mafic schist, which occurs only in the antiforms and occupies the lowermost position in the western outcrop (Fig. 10E).

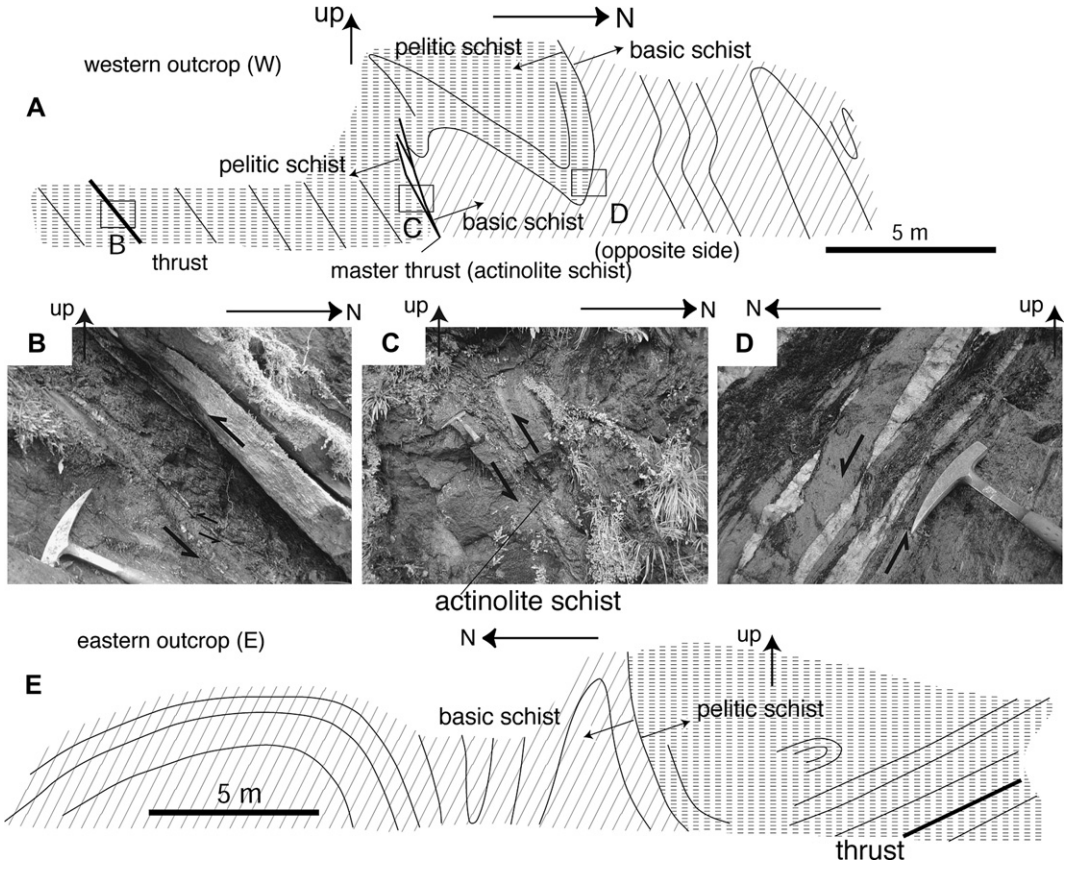


Fig. 10. D2 thrust between the oligoclase- and albite–biotite zones and associated D2 folds, in the western (A–D) and eastern (E) outcrops. (A) Cross-sectional sketch showing fault-propagation fold; (B–D) photos in rectangles in sketch A. (B) Gouge thrust in pelitic schist; thrust composed of actinolite schist. (C) N-directed asymmetric boudinage in overturned limb. Modified after Osozawa et al. (2006), fig. 9E,B–D, respectively. (E) Cross-sectional sketch showing fault-propagation fold in the eastern outcrop.

A thrust within the oligoclase–biotite zone and at the top of the marker mafic schist is easily traced (Fig. 2). The shear zone consists again of fine-grained actinolite schist. The hanging wall consists of pelitic and psammitic schists below the Asemigawa detachment fault, and asymmetrically folded with overturned limbs (Fig. 11A). The corresponding asymmetry is observed in crenulations in YZ sections (Fig. 6B). The fold geometry relative to the fault (Fig. 11A) indicates fault propagation folding.

The thrust between the albite–biotite and garnet zones (Fig. 2; Fig. 3B right, a-g) consists of an ~2 cm thick gouge and an ~5 cm shear zone. S-vergent folds with parasitic structures are well developed in the hanging wall. Biotite disappears in the footwall garnet-zone schist.

The thrust between the garnet and chlorite zones (Fig. 2; Fig. 3B, g-c) consists of a quartz veined shear zone ~2.5 m thick, with both margins comprising fault gouge. The overturned limb of a south-vergent mesoscopic antiform constitutes the hanging wall (Fig. 11B). The associated parasitic folds are, however, S-directed and concordant to the minor displacements along the axial planes (Fig. 11C), which are oblique to the master fault. The parasitic folds have an axis highly oblique to the D1 stretching lineation and bend them (see below). The footwall corresponds to the overturned northern limb of a synform, associated the N-directed parasitic folds. Garnet disappears, but albite porphyroblasts are observed in this footwall schist.

Other thrust faults are accompanied by N-plunging slickenlines (Fig. 3B right). The thrust faults consist of black gouge typically millimeters to centimeters in thickness. The shear zones are commonly associated with S-directed asymmetric folds, some showing fault propagation (Fig. 11D).

### 3.3.6. D2 folds

The majority of asymmetric folds in the Asemigawa section are D2. These are cylindrical, Class 1B to 1C (Ramsay, 1967) parallel to sub-similar, rarely kink, close to isoclinal folds (Fig. 12A,B). The D2 folds can be easily distinguished from D1 folds as they are characterized by folding of D1 schistosity at outcrop and thin section scales. In thin section, mica grains are folded (Fig. 6B), in contrast to the D1 folds whose axial planes are defined by preferential arrangement of micas (Fig. 6A). D2 folds are associated with axial planar, pressure-solution, and spaced cleavages, which overprint the pre-existing D1 schistosity (Fig. 6B). The D2 axial planes are therefore oblique to the D1 schistosity and define a D2 intersection lineation, in contrast to the D1 sheath folds whose

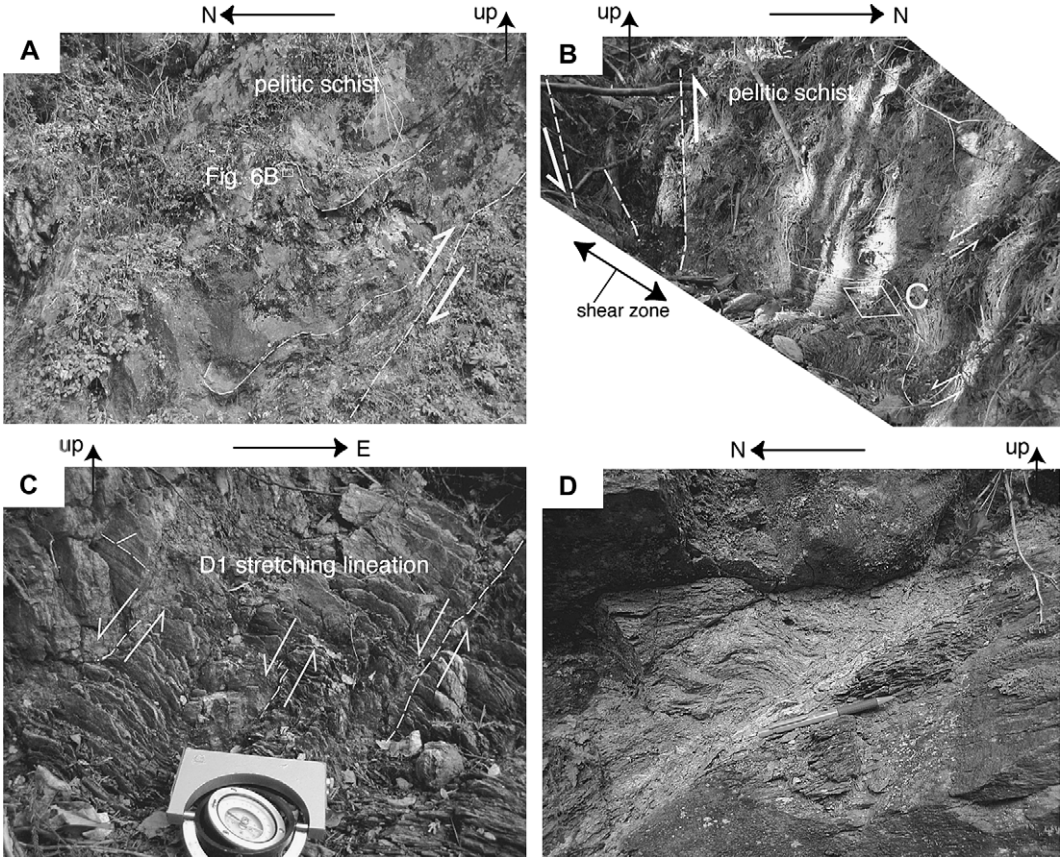


Fig. 11. (A) D2 thrust and thrust propagation fold in the oligoclase–biotite zone of lower domain. The footwall is a mafic schist. Thin section in Fig. 6B is taken from the rectangle. (B) D2 thrust between the garnet and chlorite zone and associated D2 folds. Minor thrust in the overturned limb close to the fold hinge indicates N-directed thrust-sense shear. Modified after Osozawa et al. (2006), fig. 8A. (C) Close-up of asymmetric fold, bending D1 stretching lineation (stereogram is shown in Fig. 14A). (D) Thrust propagation fold in the oligoclase–biotite zone of lower domain. Gouge is associated.

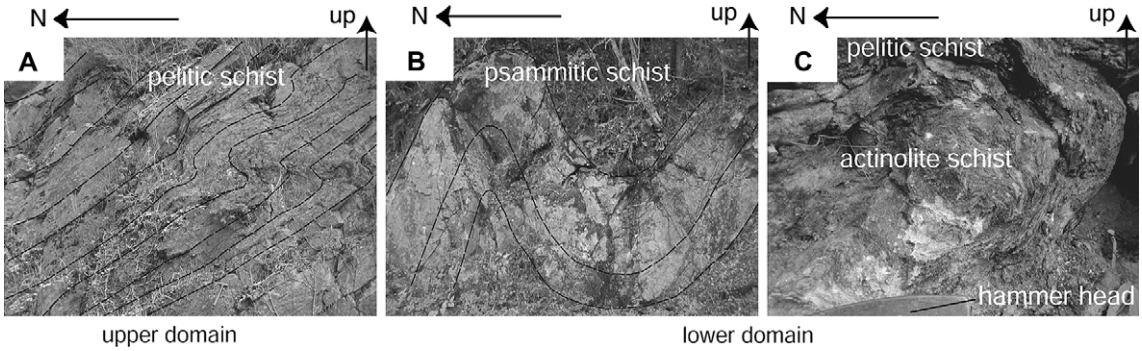


Fig. 12. D2 symmetric fold. (A) N-vergent, pelitic schist of albite–biotite zone in upper domain, and (B) S-vergent, psammitic schist of oligoclase–biotite zone in lower domain. (C) S-vergent, involving actinolite schist of albite–biotite zone in lower domain. Modified after Osozawa et al. (2006), fig. 12A.

axial planes lie within the schistosity and whose axes are parallel to the D1 stretching lineation.

D1 stretching lineations and D2 fold axes are generally subparallel, but locally highly oblique. The D1 lineations are commonly refolded (Fig. 13), but the D2 fold axes and intersection lineations are homogeneous over large areas (Fig. 3C). The small-circle girdle pattern of D1 lineations, and the correspondence of poles of small circles and D2 fold axes (Fig. 14) is consistent with the inference that D2 fold style is the result of flexural slip. In addition, striations are locally observed on the D2 folded surfaces, providing further support for fold accommodation by flexural slip. The obliqueness of D1 and D2 lineations was described by Nishikawa et al. (1994) only in the chlorite zone, but otherwise has not been recognized prior to the present work.

In the albite–biotite zone of the lower domain, we have observed folded actinolite schist, which is again lithologically similar to the rocks along the Asemigawa detachment fault. D2 P/T conditions were, therefore, lower than sub-greenschist facies, and strongly suggests that the D2 folding occurring during falling temperature conditions associated with exhumation.

A change in the vergence of D2 asymmetric folds is evident (Fig. 2), and occurs across the trace of the Asemigawa detachment fault (Fig. 2). The previous findings by Kawachi (1968) and by Wallis et al. (1992) differ from ours in the spatial distribution, mostly due to their sparse data and due to different inferences of the structural succession. An exception to the change in vergence we describe here is apparently found in the lower domain, in the overturned short limbs of first-order

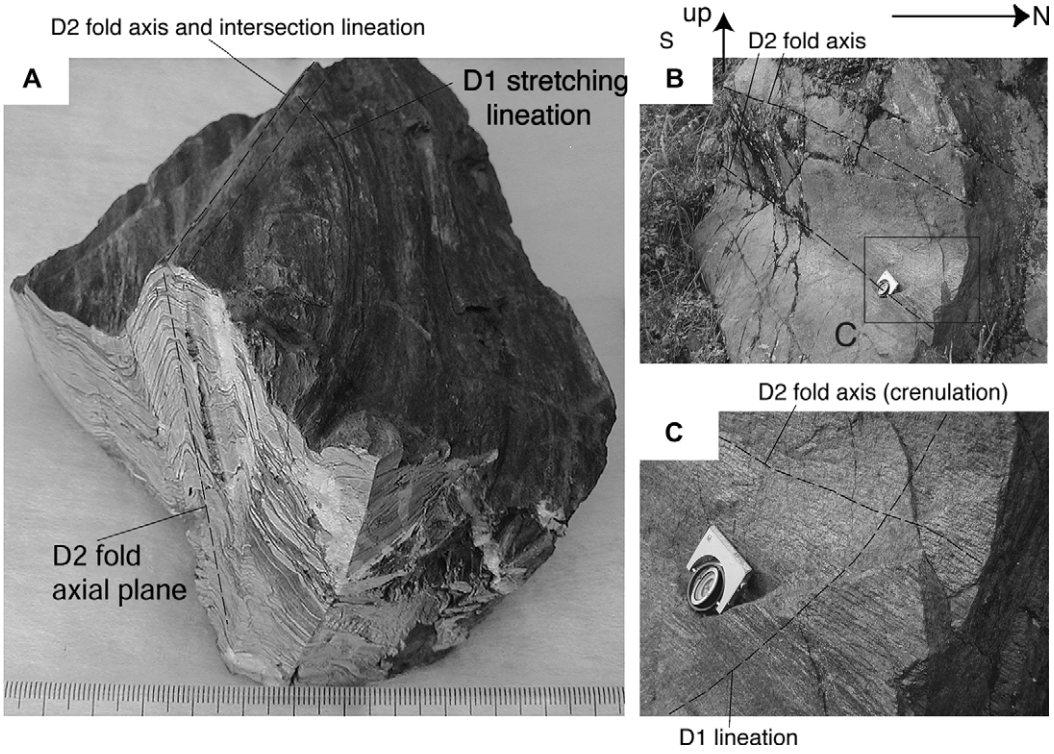


Fig. 13. D1 stretching lineations obliquely bent by D2 folding. (A) Pelitic schist, chlorite zone, and (B) key mafic schist, overturned limb in oligoclase–biotite zone in lower domain. (C) Enlarged rectangle shown in B. Modified after Osozawa et al. (2006), fig. 10A,B.

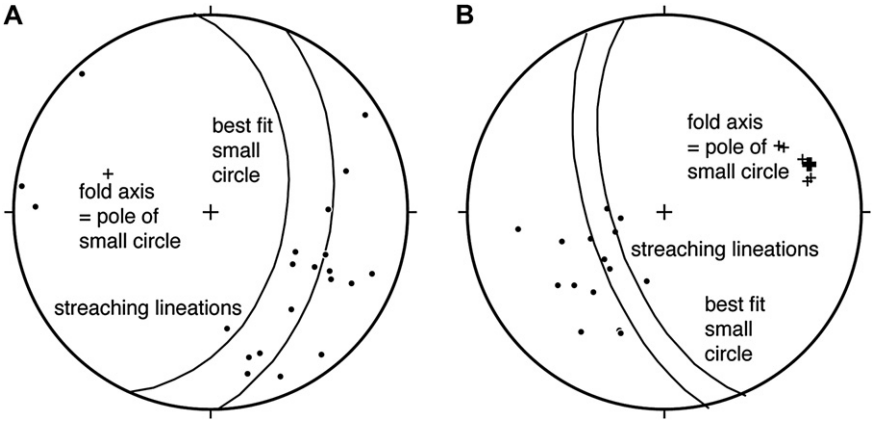


Fig. 14. Lower hemisphere and equal area projections of D1 stretching lineations, their best-fit small circles and D2 fold axes. (A) Pelitic schist of garnet zone in lower domain, hanging wall of contact thrust, shown in Fig. 11B. Modified after Osozawa et al. (2006), fig. 8B. (B) Mafic schist of oligoclase–biotite zone in lower domain, shown in Fig. 13B. Modified after Osozawa et al. (2006), fig. 10C.

folds (see above), but aside from this exception, the geometry is very consistent.

D2 folding is somewhat sporadic in the upper section, and is mostly restricted to near the thrust faults in the lower section. Consequently, most of the metamorphic sequence of the Asemigawa section escaped D2 folding and overturning with only a small tilting northwards as the main D2 effect. Specifically, the upper domain only dips at a low angle (Fig. 3A). The D0 eastward- and D1 west-directed shearing described above is, therefore, mostly preserved and not complicated by large-scale later overturning (Fig. 2).

### 3.4. D3

D3 is recognized as upright folds with a wavelength of ca. several kilometers and an E–W axis (Fig. 1). In the most downstream part of the Asemigawa section, antiforms and synforms of this type are recognized, with a wavelength in the region of 300 m (Fig. 2). The antiform is called the Sakamoto antiform by Hara et al. (1992). D2 folds are refolded by D3 folding in outcrop, shown schematically on Fig. 2, and this indicates that D3 folding is limited to gentle to open folding (Fig. 2). The D3 upright folding clearly affects the M2 thermal axis and metamorphic inversion (Fig. 1), and hence also affects the D2 normal and thrust faults.

Randomly oriented kink bands are rarely observed in outcrops and thin sections, and may be related to even later deformation rather than D3. The normal faults with strike-slip components reported by Takeshita and Yagi (2004) are also D3 or later according to the present study.

## 4. Discussion of the mechanism for metamorphic inversion and exhumation

### 4.1. Previous models

Three models have been proposed previously for the development of the metamorphic structure of the Sambagawa zone in Japan (Fig. 15). Each has major limitations and based on our new observations, we propose an alternate model here (Fig. 15D).

Banno et al. (1978) proposed that the metamorphic inversion in the Sambagawa zone occurred by major recumbent folding with a wavelength of 10 km and a southward closure (Fig. 15A). The Asemigawa section lies in the hinge of this proposed fold, corresponding to the thermal maximum of the metamorphic system. In this model, metamorphic inversion is produced in an overturned southern limb, and the original normal thermal structure is preserved in the northern limb. This model, however, would demand S-vergent parasitic folds

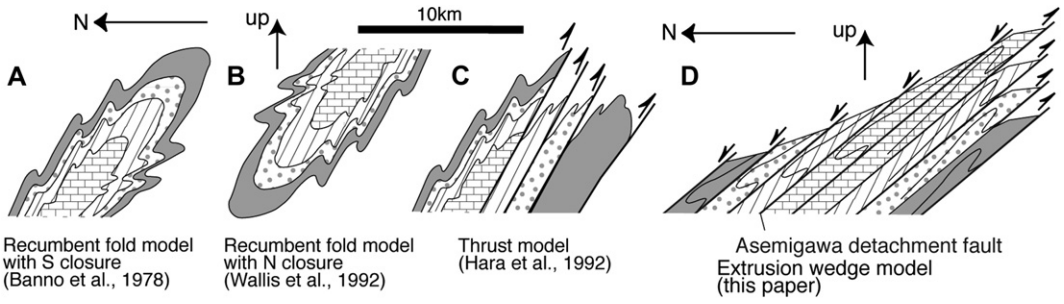


Fig. 15. Previous (A–C) and present (D) models explaining metamorphic inversion and exhumation. Modified after Osozawa et al. (2006), fig. 2. See text for details.

for the northern limb and N-vergent parasitic folds for the southern limb, which is the opposite of the observed vergence patterns for the D2 folds.

A second, more recent model suggests a recumbent fold model, but with synformal, northward closure (Fig. 15B), which is in accord with the observation that the northern and southern limbs will be accompanied by N- and S-vergent parasitic folds, respectively. Thermal inversion is expected in a subduction zone where a cold oceanic plate is being subducted, and the metamorphic inversion of the Asemigawa section can be explained as a primary feature without the tectonic overturning required by this model (Enami et al., 1994; Wallis, 1998).

A major problem with this model is the relative chronology of D1 E–W shear and the S-vergent recumbent folding with E–W axes. D1 longitudinal shear, parallel to the Sambagawa zone, is contemporaneous with the formation of stretching lineations (Faure, 1983, 1985). In the Asemigawa section, top-to-the-west shear is plausible (Wallis, 1990; Takeshita and Yagi, 2004; Fig. 2) for both the northern and southern limbs of the suspected recumbent fold. If the D2 recumbent fold with an E–W axis modifies the D1 shear with E–W sense, the shear sense in the overturned limb has to be reversed from the normal limb. This discrepancy caused Wallis (1990) to propose that westward shear and southward recumbent folding occurred simultaneously and that D1 and D2 are not distinguishable phases. However, we have shown that D1 is clearly distinguishable from D2 both in the field and in thin section. Consequently, D1 has not affected overturning to produce the metamorphic inversion. Perhaps the most important factor, however, is that no major recumbent fold is observed in the Asemigawa section. Finally, we note that in any case, this model, by itself, fails to provide a clear mechanism for deep exhumation of the complex because the E–W shear is orogen parallel and cannot easily account for large-scale exhumation.

A third model for the area is a thrust model (Fig. 15C). In this model, thrusting between the hanging wall of higher-grade metamorphic rocks and the lower-grade footwall produced the metamorphic inversion (Higashino, 1990; Hara et al., 1992). Studies by Faure (1983, 1985) are included in the thrust model. For the Asemigawa section, major thrusts would exist at the base of the oligoclase–biotite, albite–biotite, and garnet zones, respectively. One criticism with this model is the absence of a clear discontinuity of metamorphic indicators between these zones and no visible major faults in outcrop (Wallis, 1998). However, here we have described all three major D2 thrusts, bounding every metamorphic mineral zone, which eliminates this criticism. The thrust model does not, however, account for our observation of normal faults and N-vergent asymmetric folds in the upper domain, nor does it account for the presence of the Asemigawa detachment fault.

### 4.2. Extrusion wedge model

We have concluded above that a major recumbent fold does not exist in this area, based on our new findings and observations. If attention is restricted to the lower domain of the Asemigawa section, a thrust model can be applied in which the southward thrusting and S-vergent folding at the time of D2 could account for the metamorphic inversion. The highest-grade rocks of the oligoclase–biotite zone have overridden the higher-grade rocks of the albite–biotite zone, then the garnet zone, and then lowest-grade chlorite zone. The metamorphic inversion, in this case, can therefore be interpreted to be secondary and tectonic.

The upper domain of the Asemigawa section comprises the oligoclase–biotite, albite–biotite, and garnet zones, in ascending order, and possesses a normal metamorphic field gradient with lower grade rocks above. Within these zones there is also no major tectonic overturning. This succession is modified by normal faulting and N-vergent folding at the time of D2. We have recognized a major boundary fault and smaller-scale, but numerous normal faults with a northward shear.

The Asemigawa detachment fault and the normal faulting in its upper domain could play an important role in exhumation of high-grade metamorphic rocks. Recently, the importance of normal detachment faulting during tectonic denudation has been emphasized for exhumation of deep seated rocks in various tectonic settings, including subduction zones (Platt, 1986, 2000; Wernicke, 1992; Hodges et al., 1998; Ring et al., 1999; Schoonover and Osozawa, 2004).

For the lower domain of the Asemigawa section, however, thrusting is also as intense as normal faulting in the upper domain, and strongly suggests the process of an extrusion wedge, as proposed by Maruyama et al. (1996) and Ring and Reischmann (2002) for subduction zones. The extrusion wedge consists of the sheet-like high-pressure metamorphic rocks sandwiched between unmetamorphosed rocks, limited by a thrust at the footwall and by a normal fault in the hanging wall.

The pelitic schist, bounded by the Asemigawa detachment fault and the thrust fault within the oligoclase–biotite zone, constitute a metamorphic core in the extrusion wedge (Figs. 2, 15D). The northward shear in the upper domain of the Asemigawa detachment fault cannot be chronologically distinguished from the southward shear in the lower domain. To the northwest of the Asemigawa section, eclogite bodies are distributed within the Besshi unit (Fig. 1). A corresponding extrusion wedge (Okamoto, 1998; Yamamoto et al., 2004) and continuous normal fault from the Asemigawa detachment fault is expected within the eclogite body to accommodate its exhumation.

Probably the most famous extrusion wedge lies in the Himalaya (e. g., Hodges et al., 1998). The Himalaya metamorphic extrusion also has a thermal culmination, accompanied by the South Tibetan Detachment above and the coeval Main Central Thrust/Main Boundary thrust-systems below. In one model (Grujic et al., 1996), the early phase of extrusion is regarded as a ductile extrusion associated with similar folding that produced a card-pack type extrusion mechanism (Ramsey, 1967), a ductile equivalent of the brittle process we recognize for the Sambagawa extrusion. Here, the extrusion is associated with D2 flexural-slip folding and brittle faulting (Fig. 15D). Additionally, an important difference is that the Asemigawa detachment fault lies within the thermal culmination of the

Sambagawa zone, which contrasts with the South Tibetan Detachment which lies above the thermal culmination. Thus, another detachment fault, equivalent to the South Tibetan Detachment, would be expected at the northern limit of the Sambagawa zone. We suggest here that the Median Tectonic Line, which is known to have an early history as a low-angle fault (Ito et al., 1996), is a candidate for a major detachment fault (Wintsch et al., 1999) atop the subduction wedge, particularly when the effects of D3 folding are restored (Fig. 1). The base of the extrusion wedge is presumably defined by a basal thrust between the Besshi and Oboke units (Wallis, 1998).

We also emphasize that the Asemigawa detachment fault only bounds two upper extensional and lower contractional domains (Fig. 15A), and that the pressure and temperature gap across the structure is not large in comparison to the Median Tectonic Line. Nonetheless, it is sufficient to cut out significant metamorphic zones, indicating a significant component of the extrusion was accommodated along the Asemigawa detachment.

Exhumation during D1 through D2 is well constrained in the Asemigawa section and when combined with the structural and tectonic record, provides significant implications for exhumation processes from D1 to D2. Stretched actinolite schist, as a component of the Asemigawa detachment fault and other D2 faults and folds, clearly indicated that biotite zone rocks were exhumed during D1 until the system reached sub-greenschist facies conditions and progressed to D2 brittle faulting. During D1, however, motion was dominantly margin parallel as indicated by W-directed ductile shear, and progressed onwards to the S-directed D2 development of an extrusion wedge. This D1 W-directed shear and stretching has been widely ascribed to highly oblique subduction (e.g. Osozawa, 1994, 1997, 1998; Takeshita and Yagi, 2004). The kinematics of D1 and it association with oblique convergence is important because: (a) the fabrics indicate that D1 motion was dominantly margin parallel, and this motion would require a long, oblique path to produce large amounts of exhumation synchronous with D1; and (b) motion within the subduction channel during oblique convergence can be very complex, including combinations of subduction, counterflow, and margin-parallel strike-slip shear (e.g., see predictions of oblique viscous wedge models by Platt, 2000). Thus, although D1 counterflow may have led to significant exhumation, the magnitude of that exhumation need not have been large.

As an analogy to D1 kinematics of the Sambagawa, we note a similarity between the general fabric relationships in Sambagawa and the Chugach metamorphic complex of southern Alaska (e.g. see Pavlis and Sisson, 1995, 2003, for general summaries of the Chugach metamorphic complex). The low-P/high-T metamorphic history of the Chugach metamorphic complex is a grossly different thermal history than the Sambagawa, but the two complexes show a surprisingly similar kinematic history that can be, at least partially, linked to a period of oblique subduction in a forearc accretionary complex. Specifically, in the Chugach metamorphic complex, a pervasive, low-angle fabric with pronounced margin-parallel stretching lineations developed during the main metamorphic event (D2 phase of Pavlis and Sisson, 1995, 2003). In Alaska, like Sambagawa, this margin parallel stretching occurred during a period of highly-oblique convergence that drove margin-parallel strike-slip systems along the backstop of the forearc system. Significantly, this process did not produce significant exhumation in the Alaskan forearc, rather the system was dominated by margin parallel motion; e.g. most of the exposed rocks were apparently not deeply subducted, and therefore, did not experience large amounts of uplift relative to the magnitude of the horizontal motions that occurred within the system. We suspect that a similar scenario may be true of Sambagawa, that although large-scale motion occurred during D1, most of that motion was probably margin-parallel. Because this motion occurred within an obliquely convergent wedge, it is likely, based on theoretical models of Platt (2000), that part of the motion was converted to counter-flow and led to partial exhumation of the complex during D1. Nonetheless, the evidence here for the development of a D2 extrusion wedge implies that a large fraction of the Sambagawa exhumation probably occurred post-D1, during the development of extrusion wedge.

The driving mechanism for the development of the D2 extrusion wedge remains an open question. One possible mechanism is that the D2 extrusion wedge phase followed the approach and subduction of an actively spreading mid-ocean ridge, and that this led to the strong compressional stress regime and exhumed the Sambagawa and Ryoke metamorphic rocks (Osozawa, 1994, 1997, 1998), forming an extrusional wedge. Again, it is possible that the Chugach metamorphic complex could ultimately used as a further analogy to this process, because that complex was also developed directly as a consequence of ridge subduction (e.g. Sisson and Pavlis, 1993), but more work is needed on the details of the Chugach complex before this hypothesis can be fully addressed.

## 5. Conclusion

The Sambagawa high P/T metamorphic rocks of the Besshi unit were exhumed by the D2 Asemigawa detachment fault acting as a key part of an extrusional wedge. No recumbent folding and major overturning, suggested by previous models, exist in the Asemigawa section of the Besshi unit. The thermal culmination lies within the oligoclase–biotite zone in the core of the Sambagawa high P/T zone, and corresponds to the Asemigawa detachment. The upper domain includes top-to-the-N directed normal faults and N-vergent asymmetric folds, and the lower domain includes top-to-the-S directed thrust faults and S-vergent asymmetric folds. The Sambagawa extrusion wedge is comparable in scale to crustal scale extrusional folds like those seen in the Himalaya. However, the motion was accommodated by mesoscopic N- and S-directed fault-propagation folds that have parasitic folds of contrasting shear sense developed by flexural slip mechanisms. Such D2 major normal and thrust faults, which juxtapose the metamorphic mineral zones, resulted in the development of normal and inverted metamorphic gradients in the upper and lower domains of the Asemigawa detachment, respectively. D1 W-directed ductile

shear formed stretching lineations and was kinematically drastically different than D2 N–S brittle shearing. The actinolite schist in the biotite zone thus shows a D1 ductile shear zone that may have originated as counter-flow in an oblique, corner-flow system and retrograde M1 due to the partial exhumation. It was then reactivated as the D2 Asemigawa detachment, with the development of associated normal faults and some asymmetric folds.

## Acknowledgments

Bob Holdsworth, as Editor, and Timothy Needham, John Platt, and Toru Takeshita as reviewers have helped to improve the manuscript. Martin Flower helped with edits of an early draft. Mark Schoonover, Hans G.A. Lallemant, and Simon R. Wallis read the early draft of manuscript and provided helpful suggestions. Field discussion in May 2006, with Toru Takeshita, Kazuhiko Ishii, Koshi Yagi, accompanied with the second author, writing of an excursion guide-book by Geological Society of Japan (Osozawa et al., 2006), and comments by Yoshitaka Hashimoto as well as Satoshi Kanisawa were all useful for improvement of the manuscript.

## References

Abe, T., Takagi, H., Shimada, K., Kimura, S., Ikeyama, K., Miyashita, A., 2001. Ductile shear deformation of the Sambagawa metamorphic rocks in the Kanto Mountains. Journal of the Geological Society of Japan 107, 337–353 (in Japanese with English abstract).

Banno, S., Higashino, T., Otsuki, M., Itaya, T., Nakajima, T., 1978. Thermal structure of the Sanbagawa metamorphic belt in central Shikoku. Journal of Physics of the Earth 26, 345–356.

Carreras, J., Druguet, E., Griera, A., 2005. Shear-zone related folds. Journal of Structural Geology 27, 1229–1251.

Cloos, M., 1982. Flow mélanges: Numerical modeling and geologic constraints on their origin in the Franciscan subduction complex. Geological Society of America Bulletin 93, 330–345.

Enami, M., 1983. Petrology of pelitic schists in the oligoclase–biotite zone of the Sanbagawa metamorphic terrain, Japan: Phase equilibria in the highest grade zone of a high-pressure intermediate type of metamorphic belt. Journal of Structural Geology 1, 141–161.

Enami, M., Wallis, S., Banno, Y., 1994. Paragenesis of sodic pyroxene-bearing quartz schists: implications for the P-T history of the Sanbagawa belt. Contributions to Mineralogy and Petrology 116, 182–198.

Ernst, W.G., 1988. Tectonic history of subduction zones inferred from retrograde blueschist P-T paths. Geology 16, 1081–1084.

Faure, M., 1983. Eastward ductile shear during the early tectonic phase in the Sanbagawa belt. Journal of the Geological Society of Japan 89, 319–329.

Faure, M., 1985. Microtectonic evidence for eastward ductile shear in the Jurassic orogen of SW Japan. Journal of Structural Geology 7, 175–186.

Frey, M., Robinson, D., 1999. Low-Grade Metamorphism. Blackwell Science, London, pp. 313.

Grujic, D., Casey, M., Davidson, C., Hollister, L.S., Kundig, R., Pavlis, T., Schmid, S., 1996. Ductile extrusion of the higher Himalayan Crystalline in Bhutan: Evidence from quartz microfabrics. Tectonopysics 260, 21–43.

Hara, I., et al., 1992. Tectonic evolution of the Sambagawa schists and its implications in convergent margin processes. Journal of the Science of the Hiroshima University Series C 9, 495–595.

Higashino, T., 1990. Metamorphic zones of the Sambagawa metamorphic belt in central Shikoku, Japan. Journal of the Geological Society of Japan 96, 703–718.

Hodges, K., Bowring, S., Davidek, K., Hawkins, D., Krol, M., 1998. Evidence for rapid displacement on Himalayan normal faults and the importance of tectonic denudation in the evolution of mountain ranges. Geology 26, 483–486.

Ito, T., et al., 1996. Geophysical exploration of the subsurface structure of the Median Tectonic Line, East Shikoku. Journal of Geological Society of Japan 102, 346–360.

Kawachi, Y., 1968. Large-scale overturned structure in the Sambagawa metamorphic zone in central Shikoku, Japan. Journal of the Geological Society of Japan 74, 607–616.

Maruyama, S., Liou, J., Terabayashi, M., 1996. Blueschists and eclogites of the world and their exhumation. International Geology Review 38, 485–594.

Moriyama, Y., Wallis, S., 2002. Three-dimensional finite strain analysis in the high-grade part of the Sanbagawa Belt using deformed meta-conglomerate. The Island Arc 11, 111–121.

Nishikawa, O., Misawa, R., Ogawa, S., Otsuki, K., 1994. Structural analysis of low grade metamorphic rocks of Sambagawa Belt in central Shikoku, Japan. Journal of the Geological Society of Japan 100, 901–914 (in Japanese with English abstract).

Okamoto, K., 1998. Inclusion-trail geometry of albite porphyroblasts in a fold structure in the Sambagawa Belt, central Shikoku, Japan. The Island Arc 7, 283–294.

Okamoto, K., Maruyama, S., Isozaki, Y., 2000. Accretionary complex origin of the Sanbagawa, high P/T metamorphic rocks, Central Shikoku, Japan - Layer-parallel shortening structure and green-stone geochemistry. Journal of the Geological Society of Japan 106, 70–86.

Osozawa, S., 1993. Normal faults in accretionary complex formed at trench-trench-ridge triple junction, as an indicator of angle between the trench and subducted ridge. The Island Arc 2, 142–151.

Osozawa, S., 1994. Plate reconstruction based upon age data of Japanese accretionary complexes. Geology 22, 1135–1138.

Osozawa, S., 1997. The cessation of igneous activity and uplift when an actively spreading ridge is subducted beneath an island arc. The Island Arc 6, 361–371.

Osozawa, S., 1998. Ridge subduction induced orogeny, a case study of Cretaceous to Paleogene southwest Japan. In: Flower, M., et al. (Eds.), American Geophysical Union Geodynamics Series, Mantle Dynamics and Plate Interactions in East Asia. American Geophysical Union, Washington, DC, pp. 331–336.

Osozawa, S., Takeshita, T., Yagi, K., Ishii, K., 2006. Exhumation-related deformation structures of the Sambagawa metamorphic rocks, central Shikoku, Japan. Journal of Geological Society of Japan 112 (Supplement), 71–86 (in Japanese).

Otsuki, M., Banno, S., 1990. Prograde and retrograde metamorphism of hematite-bearing basic schists in the Sanbagawa belt in central Shikoku. Journal of Metamorphic Geology 8, 425–439.

Passchier, C.W., Trouw, R.A.J., 1996. Micro-Tectonics. Springer, Berlin, Heidelberg, New York, 289 pp.

Pavlis, T.L., Sisson, V.B., 1995. Tectonic processes during ridge subduction: Chugach Metamorphic Complex, southern Alaska. Geological Society of America Bulletin 107, 1333–1355.

Pavlis, T.L., Sisson, V.B., 2003. Development of a subhorizontal decoupling horizon in a transpressional system, Chugach Metamorphic Complex, Alaska: Evidence for rheological stratification of the crust. In: Sisson, V.B., Roeske, S., Pavlis, T.L. (Eds.), Geology of a Transpressional Orogen Developed during Ridge-Trench Interaction along the North Pacific Margin. Geological Society of America Special Paper 371, pp. 191–216.

Platt, J.P., 1986. Dynamics of the orogenic wedge and the uplift of high-pressure metamorphic rocks. Geological Society of America Bulletin 97, 1037–1053.

Platt, J.P., 2000. Calibrating the bulk rheology of active obliquely convergent thrust belts and forearc wedges from surface profiles and velocity distributions. Tectonics 19, 529–548.

Radvanec, M., Banno, S., Okamoto, K., 1994. Multiple stages of phengite formation in Sanbagawa schists. Mineralogy and Petrology 51, 37–48.

Ramsay, J.G., 1967. Folding and Fracturing of Rocks. McGraw Hill, New York, 568 pp.

Ring, U., Reischmann, T., 2002. The weak and superfast Cretan detachment, Greece: Exhumation at subduction rates in extruding wedges. Journal of Geological Society London 159, 225–228.

Ring, U., Brandon, M.T., Willett, S.D., Gordon, S., 1999. Exhumation processes. In: Ring, U., Brandon, M.T., Lister, G.S., Willett, S. (Eds.), Exhumation Processes: Normal Faulting, Ductile Flow and Erosion. Geological Society, London, Special Publications, vol. 154, pp. 55–86.

Robinson, P., Spear, F.S., Schumacher, J.C., Laird, J., Klein, C., Evans, B.W., Doolan, B.L., 1981. Phase relations of metamorphic amphiboles: Natural occurrence and theory. In: Veblen, D.R. (Ed.), Amphiboles: Petrology and Experimental Phase Relations. Reviews in Mineralogy 9B, pp. 1–228.

Schoonover, M., Osozawa, S., 2004. Exhumation process of the Nago subduction related metamorphic rocks, Okinawa, Ryukyu island arc. Tectonophysics 393, 221–240.

Sisson, V.B., Pavlis, T.L., 1993. Geologic consequences of plate reorganization: An example from the Eocene southern Alaska forearc. Geology 21, 913–916.

Spear, F.S., 1993. Metamorphic Phase Equilibria and Pressure-Temperature-Time Paths. Mineralogical Society of America Monograph Series, 799.

Suppe, J., 1985. Principles of Structural Geology. Prentice Hall, Englewood Cliffs, NJ, 537 pp.

Suzuki, S., Ishizuka, H., 1998. Low-grade metamorphism of the Mikabu and northern Chichibu belts in central Shikoku, SW Japan: Implications for the areal extent of the Sanbagawa low-grade metamorphism. Journal of Metamorphic Geology 16, 107–116.

Tagami, M., Takeshita, T., 1998. *c*-Axis fabrics and microstructures in quartz schist from the Sambagawa metamorphic belt, central Shikoku, Japan. Journal of Structural Geology 20, 1549–1568.

Takagi, K., Hara, I., 1979. Relationship between growth of albite porphyroblasts and deformation in a Sambagawa schist, central Shikoku, Japan. Tectonophysics 58, 113–125.

Takasu, A., Dallmeyer, R.D., 1990. 40Ar/39Ar mineral age constraints for the tectonic evolution of the Sambagawa metamorphic belt, central Shikoku, Japan: A Cretaceous accretionary prism. Tectonopysics 185, 111–139.

Takeshita, T., Ishii, K., Kanagawa, K., 2005. Flow kinematics in the deeper part of a subduction channel, as inferred from inclusion trails in plagioclase porphyroblasts from the Sambagawa metamorphic rocks, southwest Japan. Journal of Metamorphic Geology 23, 279–294.

Takeshita, T., Yagi, K., 2004. Flow patterns during exhumation of the Sambagawa metamorphic rocks, SW Japan, caused by brittle–ductile, arc parallel extension. In: Grocott, J., MacCaffrey, K.J.W., Taylor, G., Tikoff, B. (Eds.), Vertical Coupling and Decoupling in the Lithosphere. Geological Society, London, Special Publications, vol. 227, pp. 279–296.

Toriumi, M., 1985. Two types of ductile deformation/regional metamorphic belt. Tectonophysics 113, 307–326.

Underwood, M.B., Laughland, M.M., Kang, S.M., 1993. A comparison among organic and inorganic indicators of diagenesis and low-temperature metamorphism, Tertiary Shimanto Belt, Shikoku, Japan. In: Underwood, M.B., et al. (Eds.), Thermal Evolution of the Tertiary Shimanto Belt, Southwest Japan: An Example of Ridge-trench Interaction. Geological Society of America, Special Paper 273, pp. 45–62.

Wallis, S., 1990. The timing of folding and stretching in the Sambagawa Belt: the Asemigawa region, central Shikoku. Journal of the Geological Society of Japan 96, 345–352.

Wallis, S., 1995. Vorticity analysis and recognition of ductile extension in the Sanbagawa belt, SW Japan. Journal of Structural Geology 17, 1077–1093.

Wallis, S., 1998. Exhuming the Sanbagawa metamorphic belt: the importance of tectonic discontinuities. Journal of Metamorphic Geology 16, 83–95.

Wallis, S., Banno, S., Radvanec, M., 1992. Kinematics, structure and relationship to metamorphism of the east-west flow in the Sanbagawa Belt, southwest Japan. The Island Arc 1, 176–185.

Wernicke, B., 1992. Cenozoic extensional tectonics of the U.S. Cordillera. In: Burchfiel, B.C., Lipmann, P.W., Zoback, M.L. (Eds.), The Cordilleran Orogen: Conterminous US, The Geology of North America, G-3. The Geological Society of America, Boulder, CO, pp. 553–581.

Wintsch, R.P., Byrne, T., Toriumi, M., 1999. Exhumation of the Sanbagawa blueschist belt, SW Japan, by lateral flow and extrusion: Evidence from structural kinematics and retrograde P-T-t paths. In: Ring, U., Brandon, M.T., Lister, G.S., Willett, S. (Eds.), Exhumation Processes: Normal Faulting, Ductile Flow and Erosion. Geological Society, London, Special Publications, vol. 154, pp. 129–155.

Yagi, K., Takeshita, T., 2002. Regional variation in exhumation and strain rate of the high-pressure Sambagawa metamorphic rocks in central Shikoku, south-west Japan. Journal of Metamorphic Geology 20, 633–647.

Yamaji, A., 2000. The multiple inverse method: A new technique to separate stresses from heterogeneous fault-slip data. Journal of Structural Geology 22, 441–452.

Yamaji, A., 2003. Are the solutions of stress inversion correct? Visualization of their reliability and the separation of stresses from heterogeneous fault-slip data. Journal of Structural Geology 25, 241–252.

Yamamoto, H., Okamoto, K., Kaneko, Y., Terabayashi, M., 2004. Southward extrusion of eclogite-bearing mafic-ultramafic bodies in the Sanbagawa belt, central Shikoku, Japan. Tectonophysics 387, 151–168.